Hindawi Publishing Corporation
Journal of Nanomaterials
Volume 2013, Article ID 453623, 12 pages
http://dx.doi.org/10.1155/2013/453623

Research Article

Reversible Surface Properties of Polybenzoxazine/Silica Nanocomposites Thin Films

Wei-Chen Su and Shiao-Wei Kuo

Department of Materials and Optoelectronic Science, National Sun Yat-Sen University, Kaohsiung 804, Taiwan

Correspondence should be addressed to Shiao-Wei Kuo; kuosw@faculty.nsysu.edu.tw

Received 17 June 2013; Revised 2 September 2013; Accepted 16 September 2013

Academic Editor: Christoph Schick

We report the reversible surface properties (hydrophilicity, hydrophobicity) of a polybenzoxazine (PBZ) thin film through simple application of alternating UV illumination and thermal treatment. The fraction of intermolecularly hydrogen bonded O–H···O=C units in the PBZ film increased after UV exposure, inducing a hydrophilic surface; the surface recovered its hydrophobicity after heating, due to greater O–H···N intramolecular hydrogen bonding. Taking advantage of these phenomena, we prepared a PBZ/silica nanocomposite coating through two simple steps; this material exhibited reversible transitions from superhydrophobicity to superhydrophilicity upon sequential UV irradiation and thermal treatment.

1. Introduction

Surface wettability, which is controlled by the surface energy and morphology, is an important property for many solid materials [1–3]. Superhydrophobic and superhydrophilic surfaces are defined as having water contact angles (WCAs) greater than 150° and close to 0°, respectively; they have been investigated extensively because of their industrial applicability [4–8]. The preparation of a superhydrophobic surface requires the combination of a rough structure on a hydrophobic surface and a lowering of the surface energy [9, 10]; a superhydrophilic surface can be achieved through a capillary effect on a hydrophilic surface [11]. Surfaces exhibiting reversible switching between superhydrophobicity and superhydrophilicity have received much attention; they have included photoresponsive materials (e.g., ZnO, TiO_2, and SnO_2) [12–16], pH-responsive materials (e.g., poly(acrylic acid)) [17, 18], temperature-responsive polymers (e.g., poly(*N*-isopropylacrylamide)) [19], and electrical potential-responsive conducting polymer films [20, 21]. Among these materials and methods, the use of light to switch the surface wettability is particularly attractive because it can be controlled quickly [22, 23]. Organic compounds (e.g., azobenzenes) that display reversible structural changes triggered by light are employed most commonly [24, 25].

Benzoxazine monomers are heterocyclic compounds featuring an oxazine ring; they are synthesized from a primary amine, phenol, and formaldehyde. Benzoxazines can be polymerized through ring-opening polymerization in the absence of a catalyst, releasing no byproducts [26–28]. Benzoxazine resins have several attractive properties: near-zero shrinkage upon polymerization, low water absorption, high char yield, excellent dimensional stability, flame retardance, stable dielectric constants, and low surface free energies [26–33]. Polybenzoxazines (PBZs) are a relatively new class of nonfluorine, nonsilicon polymeric materials that exhibit low surface free energies as a result of strong intramolecular hydrogen bonding [34]; they have a wide range of applications as superhydrophobic surfaces [35–39] in lithographic patterning [40] and as mold-release materials in nanoimprint technology [41].

Macko and Ishida reported that carbonyl-containing species were formed when a PBZ based on bisphenol A was exposed to UV radiation under ambient conditions. The 2,6-disubstituted benzoquinone moieties released from the isopropylidene linkages of PBZ are the primary reactive sites where oxidation and cleavage occur upon UV exposure. These benzoquinone moieties decrease the fraction of intramolecular hydrogen bonding while increasing the fraction of intermolecular hydrogen bonding [42, 43]. Liao

et al. reported that the surface properties of PBZ become hydrophilic upon decreasing the fraction of intramolecular hydrogen bonds after UV exposure. Our motivation for this study was to test whether we could obtain reversible switching of the surface properties—between superhydrophobicity and superhydrophilicity—of a PBZ thin film [40].

Reversible transitions from superhydrophobicity to superhydrophilicity have been observed previously for aligned ZnO nanorod films through intelligent control over alternating UV illumination and dark storage [12, 13]. In addition, a photo-switched azobenzene thin film displaying a superhydrophobicity-to-superhydrophilicity transition has been realized, controlled through UV and visible irradiation [24, 25]. Hou and Wang reported that a polystyrene/titania (TiO_2) hybrid could also be adjusted from superhydrophilicity to superhydrophobicity by alternating UV illumination and thermal treatment with different drying temperatures [44]. Similar behavior has also been reported for a methylsilicone/phenolic resin/silica composite surface [45].

In this study, we observed reversible surface properties, controlled through alternating UV illumination and thermal treatment at different temperatures, of a pure PBZ thin film. Taking advantage of these phenomena, we also prepared a PBZ/silica nanocomposite coating through two simple steps, using a previously reported procedure [35]; this material also exhibited reversible transitions from superhydrophobicity to superhydrophilicity upon sequential UV irradiation and thermal treatment.

2. Experimental

2.1. Materials. Paraformaldehyde and allylamine were purchased from Tokyo Kasei Kogyo (Japan). Bisphenol A was supplied by the Showa (Japan). The benzoxazine monomer VB-a was prepared according to reported procedures [46, 47]. Column chromatography (eluent: EtOAc/hexane, 2 : 1) was used to separate the impurities, which were identified as unreacted phenols, amines, and benzoxazine oligomers. Silica nanoparticles (Tokusil 233G; 22-nm precipitated hydrated silica) were kindly provided by the Oriental Silicas (Taiwan).

3. Thin-Film Formation and Polymerization

A low-surface-energy thin film of PBZ was prepared from a solution of the VB-a monomer (0.5 g) in THF (10 mL) that was filtered through a 0.2 μm syringe filter and then spin-coated in a glass slide (100 × 100 × 1 mm), which was then cured in an oven at 200°C. A superhydrophobic coating comprising PBZ and silica nanoparticles on a glass slide was formed through a two-step process. First, VB-a benzoxazine (0.5 g) was mixed with the silica nanoparticles (0.75 g) in THF (10 mL). After ultrasonication in a bath for 2 h, the mixture was spin-coated (1500 rpm, 45 s) in a glass slide (100 × 100 × 1 mm) and then cured in an oven (200°C, 1 h). Subsequently, the PBZ-silica hybrid surface was modified with 0.1% (w/v) VB-a PBZ film. The VB-a benzoxazine solution was spin-coated (1500 rpm, 45 s) in a rough surface and then cured (210°C, 1 h). To produce a hydrophilic surface, the VB-a PBZ thin film was exposed (ca. 120 min) through a mask to UV radiation (265 nm) at a distance of 25 cm from the source, receiving 30 W/m^2 of radiation. The sample was then thermally cured at different temperatures in an oven to reform the superhydrophobic surface. To investigate the effects of thermal treatment, the temperature was set at 80, 100, 120, 140, 160, 180, or 200°C.

4. Characterization

A Data Physics OCA20 goniometer interfaced to image-capture software was used to measure the advancing contact angles of the samples at 25°C; a liquid drop of deionized water was injected in the polymer surface. Surface roughness profiles of the film structures were acquired using a NT-MDT solver PRO-M scanning probe microscope operated in the tapping mode. Root-mean-square (rms) roughnesses were calculated over scan areas of 5 μm × 5 μm. The chemical composition of the as-prepared surface was investigated through X-ray photoelectron spectroscopy (XPS) using a PHI 5000 VersaProbe electron spectrometer and an AlKR line excitation source with the reference of C_{1s} at 285.00 eV. The microstructures of the polymer surface and the mold were characterized using a JEOL JSM-6380 scanning electron microscope.

5. Results and Discussion

For the VB-a monomer system that had been heated at various curing temperatures (Figure 1(a)), the WCA increased upon increasing the curing temperature, from 82° at 80°C to 103° at 200°C, similar to the behavior of a previously reported BA-a PBZ system [29]. Figure 1(b) reveals that the WCA of the VB-a PBZ films decreased upon increasing the UV exposure time. After UV exposure for longer than 120 min, the WCA reached very close to 0°, corresponding to a superhydrophilic surface. This behavior arose due to the partial decrease in the degree of intramolecular hydrogen bonding and a corresponding increase in the degree of intermolecular hydrogen bonding, thereby resulting in a higher surface free energy and a greater hydrophilicity [40]. Liao et al. reported a simple method using a photomask to produce wettability patterns and wettability gradients on the surfaces of PBZ films; they also suggested that the surface free energy and hydrophilicity of these PBZ films could be controlled through a combination of thermal treatment and UV exposure to change the ratio of intra- to intermolecular hydrogen bonds [40].

Figure 2 displays the effects on the UV-exposed PBZ films after thermal treatment at various temperatures. Surprisingly, the WCA increased upon increasing the thermal treatment temperature, from 1.5° at 80°C to 102.9° at 200°C, behavior that is very similar to that observed after the first thermal curing procedure at 200°C. The wettability of this PBZ film revealed a transition from hydrophilicity to hydrophobicity upon increasing the thermal treatment temperature. Again, we used WCAs to measure the reversible switching of the PBZ

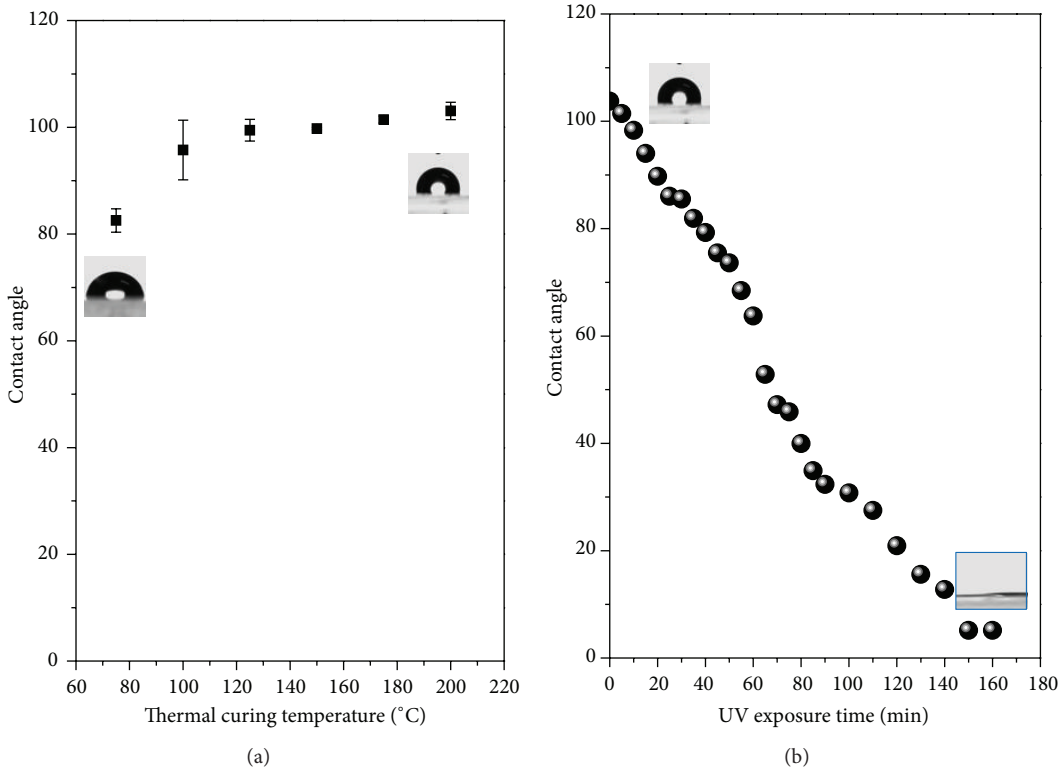

Figure 1: Variations in WCA after (a) the first thermal curing of the VB-a monomer at various temperatures and (b) the first UV exposure for various lengths of time.

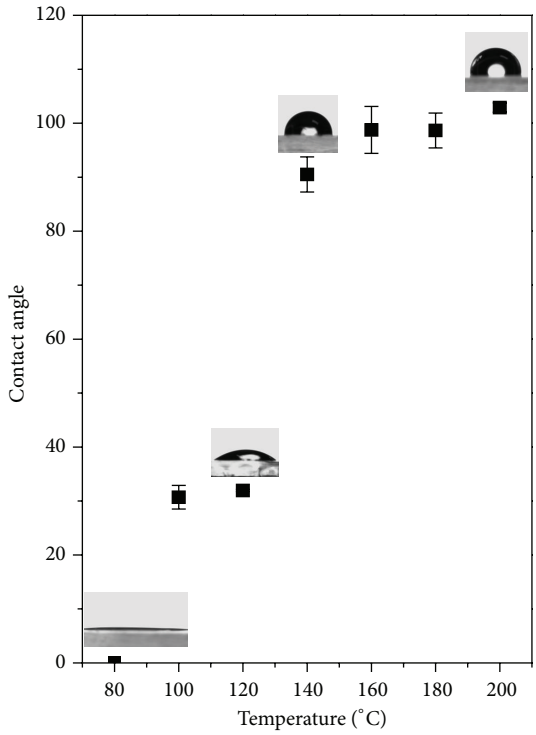

Figure 2: Variation in WCA after performing the second thermal treatment at various temperatures.

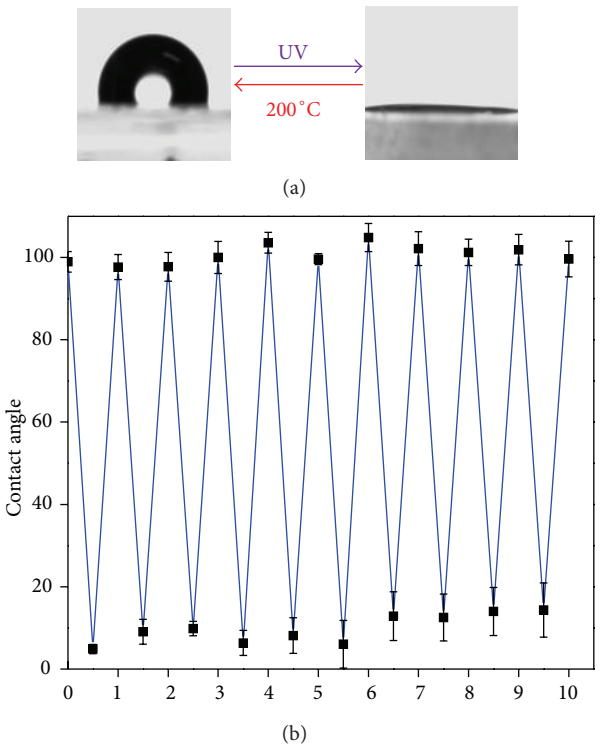

Figure 3: (a) Photographs of a water droplet on the PBZ coating before (left) and after (right) UV illumination. (b) Reversible hydrophobic-hydrophilic transitions of the as-prepared coatings through sequential alternating of UV irradiation and thermal treatment.

film between its hydrophilic and hydrophobic states. Figure 3 displays a WCA of approximately 100° for the PBZ film after initial thermal treatment at 200°C. After UV irradiation for 2 h, the WCA decreased to 2 ± 2°, a clear transformation in the wettability of this PBZ film from hydrophobicity to hydrophilicity. After UV exposure, we heated this sample again at 200°C for 1 h, regaining the hydrophobicity of its surface. We could repeat this process several times, obtaining good reversibility of the surface wettability. To determine the factors responsible for these transitions, we used XPS to investigate the chemical structures of the surface components of the PBZ films.

Figures 4 and 5 present XPS analyses of the compositions of a PBZ film after alternating UV illumination and thermal treatment. Table 1 lists the peak assignments of the C 1s and O 1s signals as well as the curve fitting data [48, 49]. Let us first consider the C=O peaks in both the C 1s (288.5 eV) and O 1s (531.4 eV) spectra in Figures 4 and 5. After the first thermal treatment procedure, the C=O peaks were not detectable in either the C 1s or O 1s spectrum; the area fractions of the C=O peaks increased, however, after UV irradiation. For example, the area fraction of the C=O peak at 288.5 eV in Figure 4(b) increased significantly (to 16.62%) after UV exposure, relative to that in Figure 4(a) without UV exposure. This result is consistent with Ishida's report: that carbonyl-containing species are formed when bisphenol A-based PBZ is exposed to UV radiation [17]. These benzoquinone moieties decrease the fraction of intramolecular hydrogen bonds while increasing the fraction of intermolecular O–H···O=C hydrogen bonds, thereby inducing a hydrophilic surface for the PBZ film. After we subjected the UV-exposed PBZ film to thermal treatment, the area fraction of the C=O peak at 288.5 eV decreased (to 9.18%; Figure 4(c)). Again, decreasing the fraction of intermolecular hydrogen bonding enhanced the hydrophobic surface properties. Finally, a further application of UV exposure significantly increased the area fraction of the C=O peak at 288.5 eV (to 19.14%; Figure 4(d)), again inducing hydrophilic surface properties. Figure 5 reveals similar trends for the C=O peaks in the O 1s spectra.

The physical interactions among the PBZ polymer chains, mainly through intramolecular hydrogen bonding of the OH groups with the nitrogen atoms, as depicted in Scheme 1, have a critical effect on the properties of these materials [40]. Let us turn our attention to the fraction of intramolecularly hydrogen bonded O–H···N units in the PBZ film, based on Figure 5. The signal at 536.5 eV for the intramolecularly hydrogen bonded O–H···N units in the PBZ film disappeared after UV exposure (area fraction: 0%; Figure 5(b)), relative to its value of 5.63% in Figure 5(a) for the sample that had not been subjected to UV exposure. After thermal treatment of the UV-exposed PBZ film, the area fraction of the O–H···N peak at 536.5 eV in Figure 5(c) increased again to 3.05%; increasing the fraction of intramolecular hydrogen bonds again enhanced the hydrophobic surface properties. Finally, further UV exposure resulted again in the disappearance of the O–H···N peak in Figure 5(d) (area fraction: 0%), thereby inducing hydrophilic surface properties once again. Therefore, the reversible switching of the wetting behavior of the PBZ film arose from the reversible chemical structures formed (cf. Scheme 1) upon alternating UV illumination and thermal treatment. Decreasing the fraction of intramolecular hydrogen bonds while increasing the fraction of intermolecular hydrogen bonds through UV exposure, as a means of inducing hydrophilic surface properties for PBZ films, has been widely discussed previously [15]. In this present case, our XPS analyses suggested that the reversible switching of the surface properties appeared to arise from a partial increase in the fraction of intramolecularly hydrogen bonded O–H···N units after UV exposure and a partial decrease in the fraction of intermolecularly hydrogen bonded O–H···O=C units after subsequent thermal treatment.

Table 2 lists the atomic percentages in the coatings after treatment under the various conditions. The ratio of N atoms was 1.5% after the first thermal treatment procedure; it increased to 4.9% after the first UV exposure. Because these N atoms each have a lone pair of electrons, they would undergo intermolecular interactions with water; therefore, we would expect a higher percentage of N atoms on the surface to induce hydrophilicity. After we had heated the UV-irradiated coating at 200°C for 1 h, the ratio of N atoms decreased, consistent with the hydrophilic surface becoming hydrophobic once again. After a second bout of UV exposure, the ratio of N atoms increased again, thereby again inducing the hydrophilic surface properties.

The ability to control the WCA of this PBZ surface through irradiation with UV light suggested the intriguing

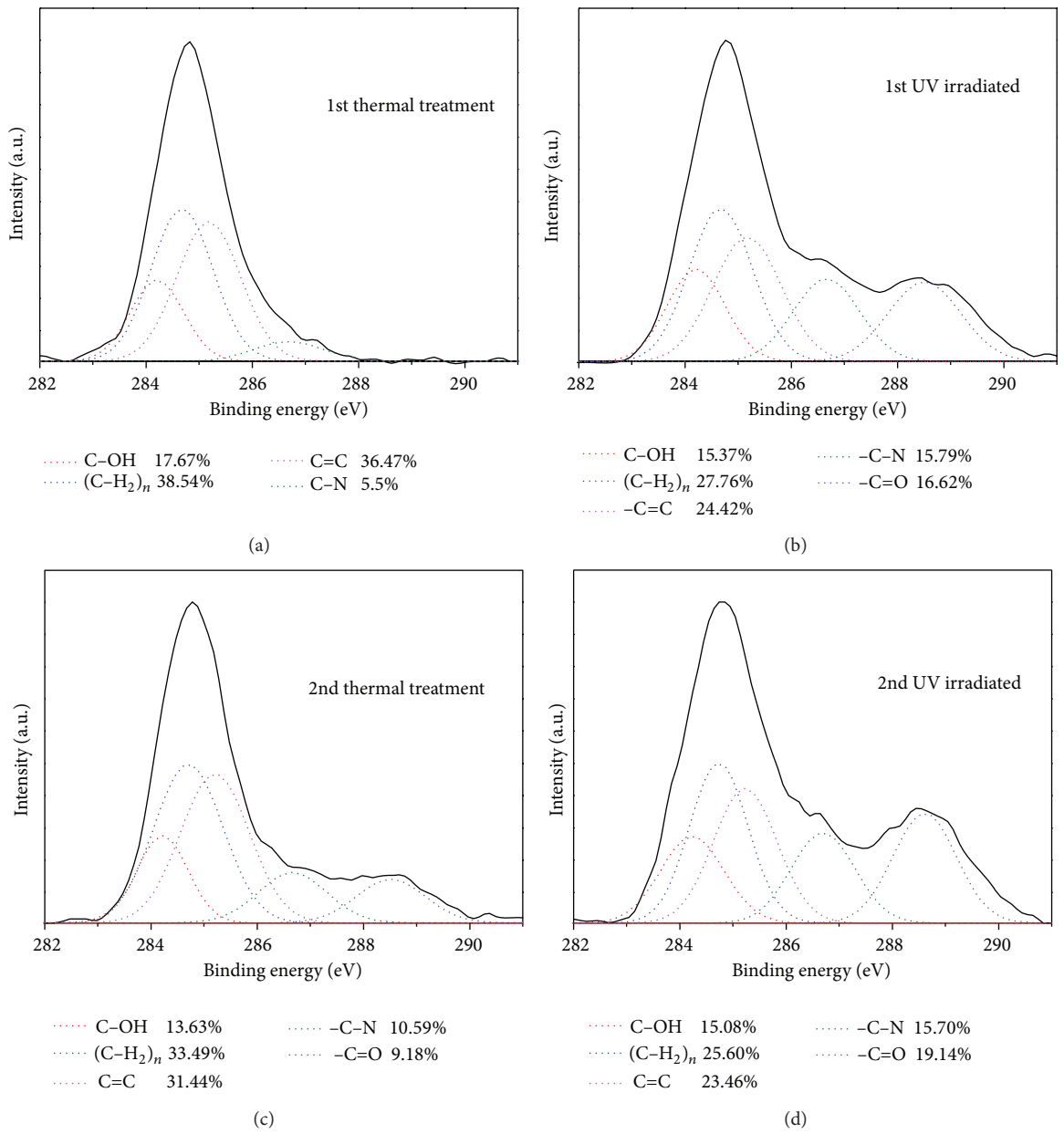

Figure 4: XPS spectra (C 1s peaks) of the PBZ film after its (a) first thermal treatment at 200°C for 1 h, (b) first UV irradiation for 2 h, (c) second thermal treatment at 200°C for 1 h, and (d) second UV irradiation for 2 h.

possibility of using this system to prepare materials with properties varying from superhydrophobicity and superhydrophilicity. Toward this goal, we used a simple two-step method to prepare a PBZ/silica nanocomposite coating, based on a previously reported procedure [35]. We obtained a superhydrophobic coating of this material on a glass slide after combining the VB-a benzoxazine monomer with silica nanoparticles in solution, spin-coating in a glass slide, and then curing. We then further modified the resulting rough surface of the PBZ-silica hybrid thin film with a thin film of the pure VB-a PBZ.

Figure 6(a) presents top-view scanning electron microscopy (SEM) images of the as-prepared super-hydrophobic surface on a glass slide. This superhydrophobic PBZ surface had a rough surface possessing both micro- and nanoscale binary structures. Each microisland (300–700 nm) on the PBZ surface was covered with nanospheres (20–60 nm); this structure dramatically increased the surface roughness and formed composite interfaces in which air could become trapped within the grooves beneath the liquid, thereby inducing superhydrophobicity. The inset to Figure 6(a) displays a spherical water droplet having a WCA of 158° on

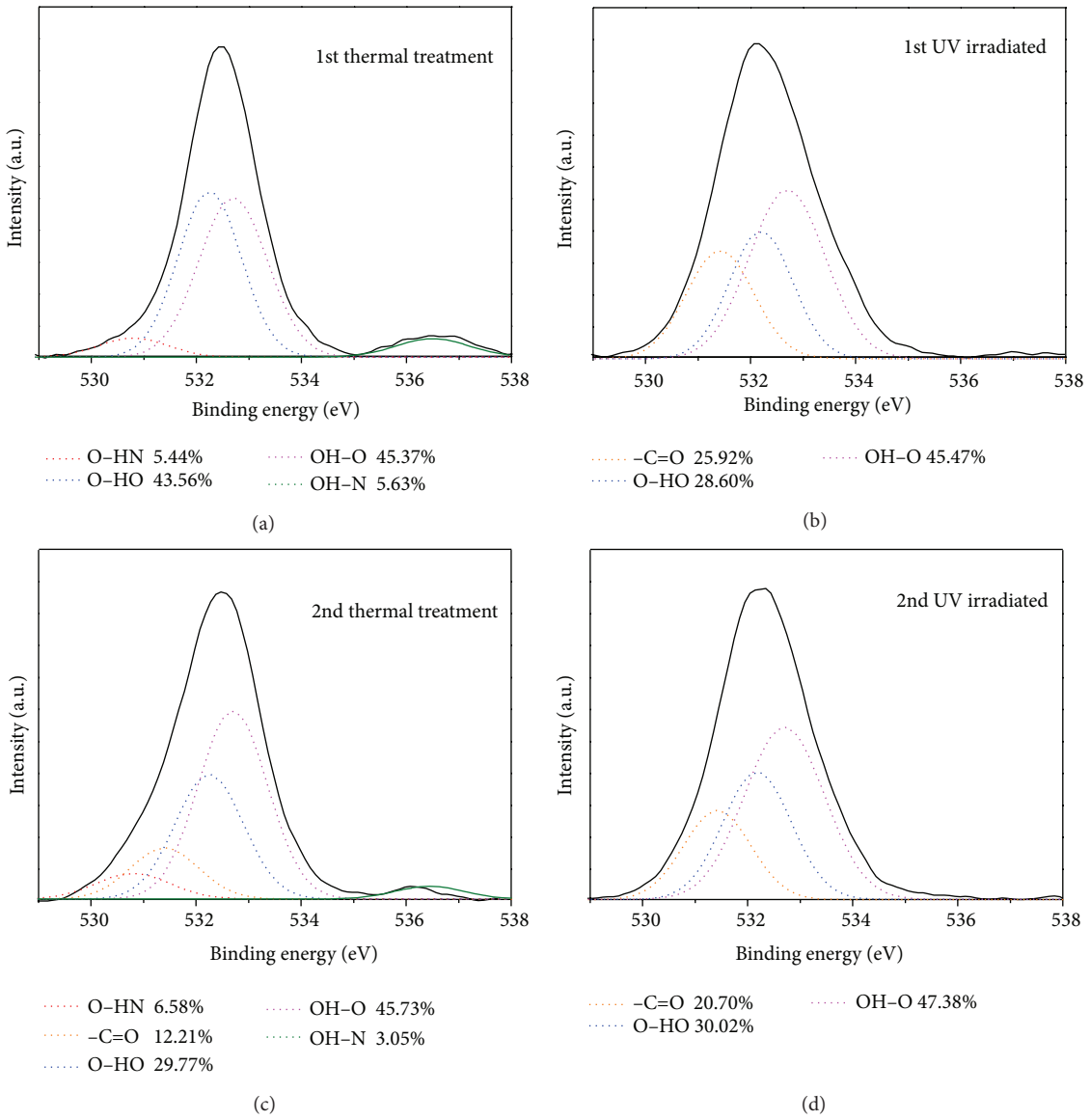

Figure 5: XPS spectra (O 1s peaks) of the PBZ film after its (a) first thermal treatment at 200°C for 1 h, (b) first UV irradiation for 2 h, (c) second thermal treatment at 200°C for 1 h, and (d) second UV irradiation for 2 h.

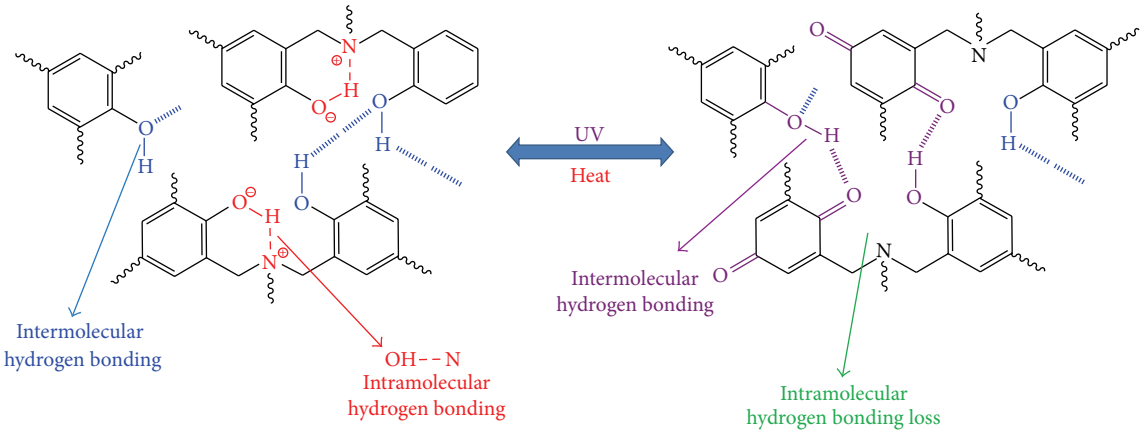

Scheme 1: Possible reversible chemical structures formed upon alternating UV irradiation and thermal treatment.

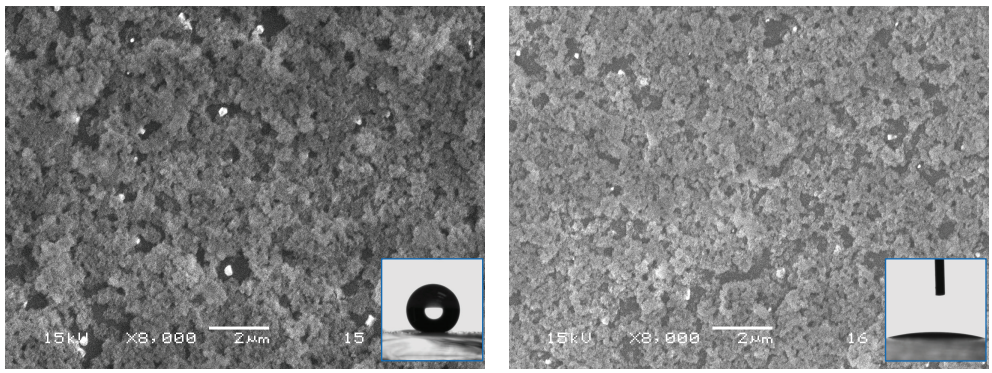

(a) (b)

Figure 6: SEM images of the PBZ-silica hybrid surface modified with VB-a PBZ (a) before and (b) after UV exposure. Inset: photograph of a water droplet on the surface.

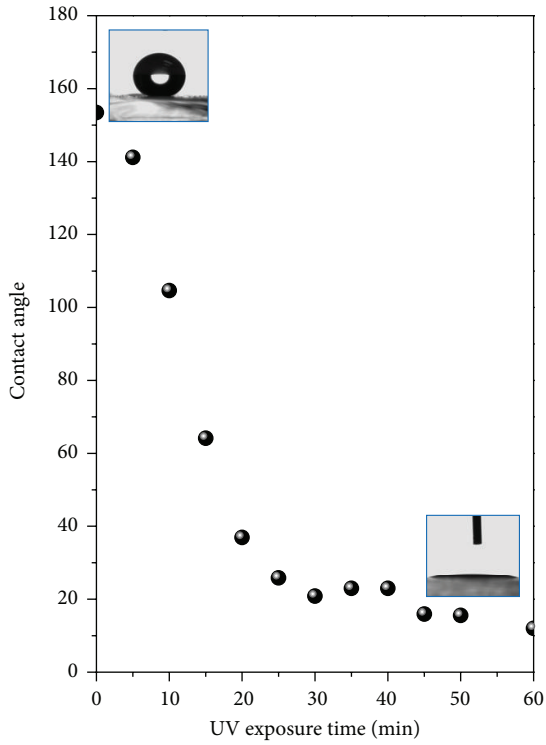

Figure 7: WCAs of the PBZ-silica hybrid surface modified with VB-a PBZ after the first UV exposure process for various lengths of time.

this surface. After UV exposure for longer than 60 min, this WCA reached very close to 0°, corresponding to a superhydrophilic surface (Figure 7). Again, we believe that a partial decrease in the degree of intramolecular hydrogen bonding and a corresponding partial increase in the fraction of intermolecular hydrogen bonding resulted in a higher surface free energy and, therefore, a higher degree of hydrophilicity in the PBZ/silica hybrid system. In addition, this superhydrophilic PBZ surface had the same rough surface, possessing both micro- and nanoscale binary structures, as that of the superhydrophobic material (cf. Figures 6(b) and 8); thus, the morphology did not change after UV exposure or thermal treatment, as confirmed through AFM analyses. The WCA of the PBZ surface after thermal treatment was 153 ± 3.2°; subsequent UV exposure decreased the WCA to 12 ± 2.3°, but it returned to the superhydrophobic state after thermal treatment once again. We could repeat the reversible switching of the surface wettability several times with good reversibility (Figure 9).

In order to realize the wetting phenomena between water droplet and PBZ/silica nanocomposite coating, we measured the advancing and receding contact angles (ARCA) by means of Needle-Syringe Injection method. In Figure 10, the WCAs and the Base Diameters (BDs) are plotted against the droplet volume when the drop is inflated and then deflated. The sessile drops are inflated with water injection rate of 0.5 μL/s

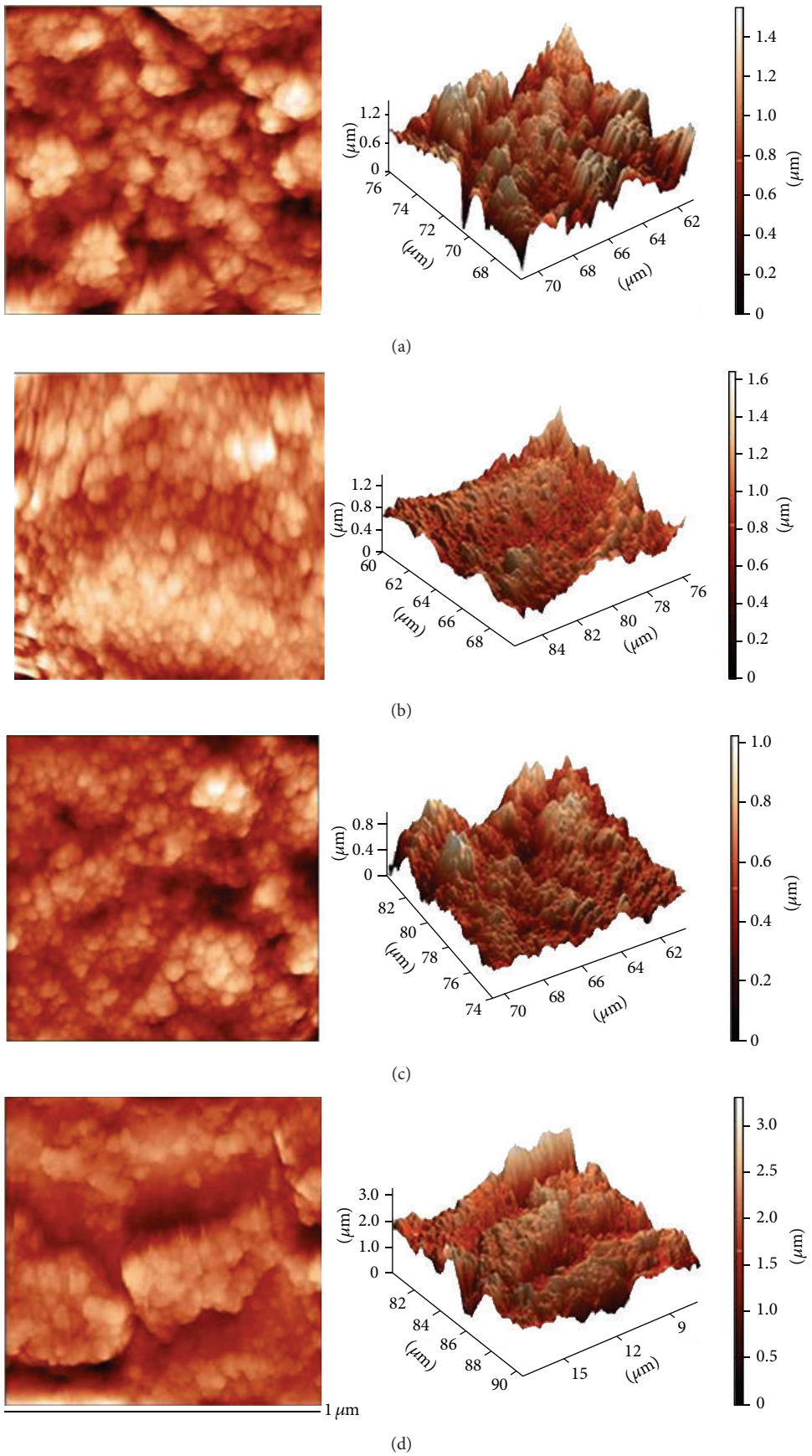

Figure 8: AFM images of the PBZ-silica hybrid surface modified with VB-a PBZ after its (a) first thermal treatment at 200°C for 1 h, (b) first UV irradiation for 1 h, (c) second thermal treatment at 200°C for 1 h, and (d) second UV irradiation for 1 h.

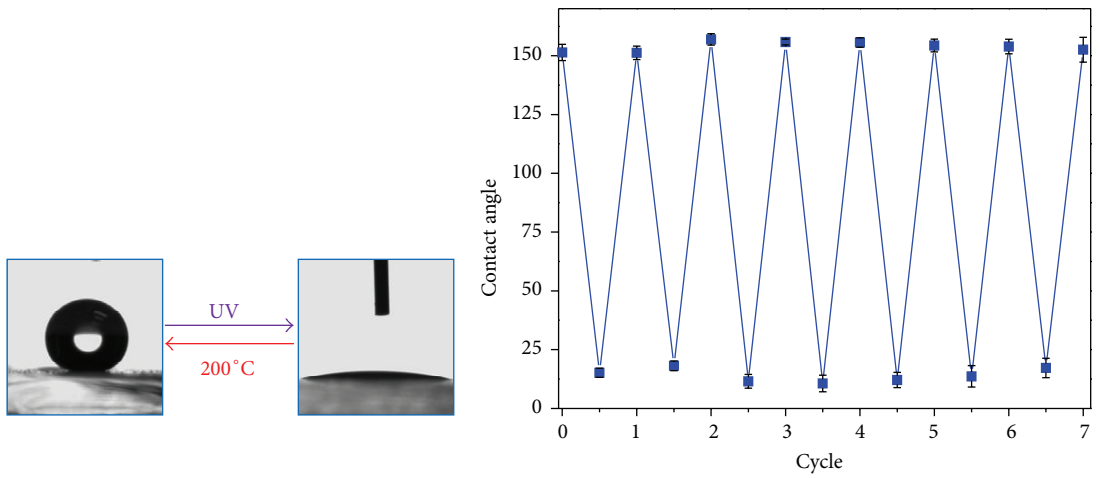

FIGURE 9: (a) Photographs of a water droplet on the PBZ-silica hybrid surface modified with a VB-a PBZ coating before (left) and after (right) UV illumination. (b) Reversible superhydrophobic-superhydrophilic transitions of the as-prepared coating upon sequential alternating of UV irradiation and thermal treatment.

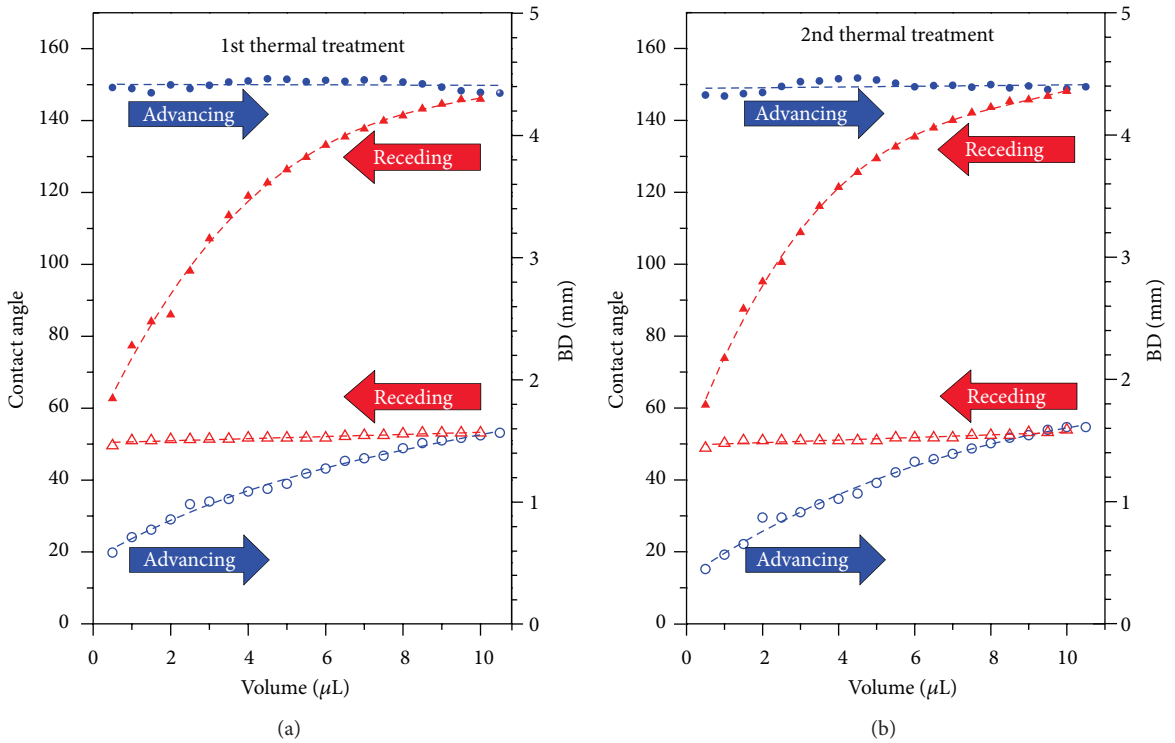

FIGURE 10: The change of WCA and BD versus the volume as the droplet is inflated and then deflated on the PBZ-silica hybrid surface: (a) first thermal treatment at 200°C for 1 h, (b) second treatment at 200°C for 1 h.

and so are the drops deflated with suction rate of 0.5 μL/s. In Figure 9, most of the static CAs of water droplets with volume of 3 μL on the PBZ/silica nanocomposite coating show superhydrophobicity (≧150°), and it is quite similar to the WCA of lotus leaf. The high water repellency of lotus leaf should be attributed to the micro- and nanoscopic structure of the leaf surface. However, Figure 10 reveals a large WCA hysteresis in our case of PBZ/silica system. Although the advancing angle of water drops can be as high as 150°, the receding angle gradually decreases to about 60° as the drop volume is deflated to less than 0.5 μL. The WCA hysteresis is very significant with $\Delta\theta \geqq 90^\circ$ in consequence of the

Table 1: Fitting data from the XPS analyses.

XPS region	Peak assignment	Binding energy (eV)	First thermal treatment A_f (%)	First UV treatment A_f (%)	Second thermal treatment A_f (%)	Second UV treatment A_f (%)
C 1s	COH	284.2	17.67	15.37	13.63	15.08
	$(CH_2)_n$	284.7	38.54	27.77	33.49	25.60
	C=C	285.2	36.47	24.44	31.44	23.46
	C–N	286.7	5.5	15.79	10.59	15.70
	C=O	288.5	—	16.62	9.18	19.14
O 1s	O···HN	530.8	5.44	—	6.58	—
	C=O	531.4	—	25.92	12.21	20.70
	O···HO	532.2	43.56	28.60	29.77	30.02
	OH···O	532.7	45.37	45.47	45.73	47.38
	OH···N	536.5	5.63	—	3.05	—

Table 2: Surface atomic abundances of the PBZ films.

Sample	C 1s (%)	N 1s (%)	O 1s (%)
First thermal treatment	63.2	1.5	35.4
First UV treatment	61.1	4.9	34.0
Second thermal treatment	50.1	2.9	47.0
Second UV treatment	54.4	6.2	39.4

BDs and also obviously exhibits pinning phenomena at the contact line during deflation. This result is similar to the case of scallion and garlic leaves [50], which exist rough surface of microscopic architecture and hydrophilic chemical defects. Likewise, in the PBZ/silica nanocomposite films, both low surface energy PBZ and silica caused roughness construct the superhydrophobicity, and the hydroxyl groups in PBZ become the hydrophilic defects which dominate the WCA hysteresis.

6. Conclusions

A PBZ/silica nanocomposite coating, prepared using a simple two-step method, exhibits reversible transitions from superhydrophobicity to superhydrophilicity and back again upon sequential UV irradiation and thermal treatment. We prepared a superhydrophobic PBZ film after introducing silica nanoparticles possessing micro- and nanoscale binary structure; it exhibited a large reversible contact angle of approximately 140°—seven times larger than that of the corresponding flat PBZ film—that could be switched through the application of sequential UV irradiation and thermal treatment. Based on XPS analyses, the fraction of intermolecularly hydrogen bonded O–H···O=C units increased after UV exposure, resulting in a PBZ film with a hydrophilic surface. The hydrophobicity of the surface returned after heating this film at 200°C, due to an increase in the degree of intramolecular O–H···N hydrogen bonding in the PBZ film. Furthermore, the ARCA experiments help us to figure out the wetting model in PBZ/silica system which is a superhydrophobic surface with serious hysteresis. We suspect that the materials exhibiting reversible WCAs reported herein might have potential new applications in lithographic patterning systems.

Acknowledgments

This study was supported financially by the National Science Council, Taiwan, under Contracts NSC 100-2221-E-110-029-MY3 and NSC 101-2628-E-110-003. The authors do not have a direct financial relation with Tokyo Kasei Kogyo, Showa Chemical Co., and Oriental Silicas that might lead to a conflict of interests for any of the authors.

References

[1] D. Yoo, S. S. Shiratori, and M. F. Rubner, "Controlling bilayer composition and surface wettability of sequentially adsorbed multilayers of weak polyelectrolytes," *Macromolecules*, vol. 31, no. 13, pp. 4309–4318, 1998.

[2] J. H. Park, Z. Schwartz, R. Olivares-Navarrete, B. D. Boyan, and R. Tannenbaum, "Enhancement of surface wettability via the modification of microtextured titanium implant surfaces with polyelectrolytes," *Langmuir*, vol. 27, no. 10, pp. 5976–5985, 2011.

[3] H. Xia, F. Xia, Y. Tang et al., "Tuning surface wettability through supramolecular interactions," *Soft Matter*, vol. 7, no. 5, pp. 1638–1640, 2011.

[4] X. Zhang, F. Shi, J. Niu, Y. Jiang, and Z. Wang, "Superhydrophobic surfaces: from structural control to functional application," *Journal of Materials Chemistry*, vol. 18, no. 6, pp. 621–633, 2008.

[5] X. Hong, X. Gao, and L. Jiang, "Application of superhydrophobic surface with high adhesive force in no lost transport of superparamagnetic microdroplet," *Journal of the American Chemical Society*, vol. 129, no. 6, pp. 1478–1479, 2007.

[6] H. Yabu and M. Shimomura, "Single-step fabrication of transparent superhydrophobic porous polymer films," *Chemistry of Materials*, vol. 17, no. 21, pp. 5231–5234, 2005.

[7] D. Öner and T. J. McCarthy, "Ultrahydrophobic surfaces. Effects of topography length scales on wettability," *Langmuir*, vol. 16, no. 20, pp. 7777–7782, 2000.

[8] H. Y. Erbil, A. L. Demirel, Y. Avci, and O. Mert, "Transformation of a simple plastic into a superhydrophobic surface," *Science*, vol. 299, no. 5611, pp. 1377–1380, 2003.

[9] N. Zhao, J. Xu, Q. Xie et al., "Fabrication of biomimetic superhydrophobic coating with a micro-nano-binary structure," *Macromolecular Rapid Communications*, vol. 26, no. 13, pp. 1075–1080, 2005.

[10] X. M. Li, D. Reinhoudt, and M. Crego-Calama, "What do we need for a superhydrophobic surface? A review on the recent progress in the preparation of superhydrophobic surfaces," *Chemical Society Reviews*, vol. 36, no. 8, pp. 1350–1368, 2007.

[11] X. Yu, Z. Wang, Y. Jiang, F. Shi, and X. Zhang, "Reversible pH-responsive surface: from superhydrophobicity to superhydrophilicity," *Advanced Materials*, vol. 17, no. 10, pp. 1289–1293, 2005.

[12] X. Feng, L. Feng, M. Jin, J. Zhai, L. Jiang, and D. Zhu, "Reversible super-hydrophobicity to super-hydrophilicity transition of aligned ZnO nanorod films," *Journal of the American Chemical Society*, vol. 126, no. 1, pp. 62–63, 2004.

[13] H. Liu, L. Feng, J. Zhai, L. Jiang, and D. Zhu, "Reversible wettability of a chemical vapor deposition prepared ZnO film between superhydrophobicity and superhydrophilicity," *Langmuir*, vol. 20, no. 14, pp. 5659–5661, 2004.

[14] W. Zhu, X. Feng, L. Feng, and L. Jiang, "UV-Manipulated wettability between superhydrophobicity and superhydrophilicity on a transparent and conductive SnO2 nanorod film," *Chemical Communications*, no. 26, pp. 2753–2755, 2006.

[15] K. Nakata, S. Nishimoto, Y. Yuda, T. Ochiai, T. Murakami, and A. Fujishima, "Rewritable superhydrophilic-superhydrophobic patterns on a sintered titanium dioxide substrate," *Langmuir*, vol. 26, no. 14, pp. 11628–11630, 2010.

[16] A. Borras, A. Barranco, and A. R. González-Elipe, "Reversible superhydrophobic to superhydrophilic conversion of Ag@TiO_2 composite nanofiber surfaces," *Langmuir*, vol. 24, no. 15, pp. 8021–8026, 2008.

[17] J. Zhou, G. Wang, J. Hu, X. Lu, and J. Li, "Temperature, ionic strength and pH induced electrochemical switching of smart polymer interfaces," *Chemical Communications*, no. 46, pp. 4820–4822, 2006.

[18] F. Xia, L. Feng, S. Wang et al., "Dual-responsive surfaces that switch between superhydrophilicity and superhydrophobicity," *Advanced Materials*, vol. 18, no. 4, pp. 432–436, 2006.

[19] T. Sun, G. Wang, L. Feng et al., "Reversible switching between superhydrophilicity and superhydrophobicity," *Angewandte Chemie*, vol. 43, no. 3, pp. 357–360, 2004.

[20] L. Xu, W. Chen, A. Mulchandani, and Y. Yan, "Reversible conversion of conducting polymer films from superhydrophobic to superhydrophilic," *Angewandte Chemie*, vol. 44, no. 37, pp. 6009–6012, 2005.

[21] J. Lahann, S. Mitragotri, T. Tran et al., "A reversibly switching surface," *Science*, vol. 299, no. 5605, pp. 371–374, 2003.

[22] H. S. Lim, D. Kwak, Y. L. Dong, G. L. Seung, and K. Cho, "UV-driven reversible switching of a roselike vanadium oxide film between superhydrophobicity and superhydrophilicity," *Journal of the American Chemical Society*, vol. 129, no. 14, pp. 4128–4129, 2007.

[23] H. S. Lim, J. T. Han, D. Kwak, M. Jin, and K. Cho, "Photoreversibly switchable superhydrophobic surface with erasable and rewritable pattern," *Journal of the American Chemical Society*, vol. 128, no. 45, pp. 14458–14459, 2006.

[24] W. Jiang, G. Wang, Y. He et al., "Photo-switched wettability on an electrostatic self-assembly azobenzene monolayer," *Chemical Communications*, no. 28, pp. 3550–3552, 2005.

[25] B. Xin and J. Hao, "Reversibly switchable wettability," *Chemical Society Reviews*, vol. 39, no. 2, pp. 769–782, 2010.

[26] C. P. R. Nair, "Advances in addition-cure phenolic resins," *Progress in Polymer Science*, vol. 29, no. 5, pp. 401–498, 2004.

[27] N. N. Ghosh, B. Kiskan, and Y. Yagci, "Polybenzoxazines-New high performance thermosetting resins: synthesis and properties," *Progress in Polymer Science*, vol. 32, no. 11, pp. 1344–1391, 2007.

[28] H. Ishida and D. J. Allen, "Physical and mechanical characterization of near-zero shrinkage polybenzoxazines," *Journal of Polymer Science B*, vol. 34, no. 6, pp. 1019–1030, 1996.

[29] C. F. Wang, Y. C. Su, S. W. Kuo, C. Huang, Y. Sheen, and F. Chang, "Low-surface-free-energy materials based on polybenzoxazines," *Angewandte Chemie*, vol. 45, no. 14, pp. 2248–2251, 2006.

[30] S. W. Kuo, Y. C. Wu, C. F. Wang, and K. U. Jeong, "Preparing low-surface-energy polymer materials by minimizing intermolecular hydrogen-bonding interactions," *Journal of Physical Chemistry C*, vol. 113, no. 48, pp. 20666–20673, 2009.

[31] L. Qu and Z. Xin, "Preparation and surface properties of novel low surface free energy fluorinated silane-functional polybenzoxazine films," *Langmuir*, vol. 27, no. 13, pp. 8365–8370, 2011.

[32] C. H. Lin, S. L. Chang, T. Y. Shen, Y. S. Shih, H. T. Lin, and C. F. Wang, "Flexible polybenzoxazine thermosets with high glass transition temperatures and low surface free energies," *Polymer Chemistry*, vol. 3, no. 4, pp. 935–945, 2012.

[33] Y. C. Wu and S. W. Kuo, "Synthesis and characterization of polyhedral oligomeric silsesquioxane (POSS) with multifunctional benzoxazine groups through click chemistry," *Polymer*, vol. 51, no. 17, pp. 3948–3955, 2010.

[34] C. F. Wang, F. C. Chang, and S. W. Kuo, "Surface properties of polybenzoxazines," in *Handbook of Polybenzoxazine*, H. Ishida and T. Agag, Eds., chapter 33, pp. 579–593, Elsevier, Amsterdam, The Netherlands, 2011.

[35] C. F. Wang, Y. T. Wang, P. H. Tung et al., "Stable superhydrophobic polybenzoxazine surfaces over a wide pH range," *Langmuir*, vol. 22, no. 20, pp. 8289–8292, 2006.

[36] C. S. Liao, C. F. Wang, H. C. Lin, H. Chou, and F. Chang, "Fabrication of patterned superhydrophobic polybenzoxazine hybrid surfaces," *Langmuir*, vol. 25, no. 6, pp. 3359–3362, 2009.

[37] C. F. Wang, S. F. Chiou, F. H. Ko et al., "Fabrication of biomimetic super-amphiphobic surfaces through plasma modification of benzoxazine films," *Macromolecular Rapid Communications*, vol. 27, no. 5, pp. 333–337, 2006.

[38] A. Raza, Y. Si, X. Wang et al., "Novel fluorinated polybenzoxazine-silica films: chemical synthesis and superhydrophobicity," *RSC Advances*, vol. 2, no. 33, pp. 12804–12811, 2012.

[39] H. C. Lin, H. L. Chang, C. F. Wang, C. F. Huang, and F. C. Chang, "Polybenzoxazine-silica hybrid surface with environmentally responsive wettability behavior," *Journal of Adhesion Science and Technology*, vol. 23, no. 4, pp. 503–511, 2009.

[40] C. S. Liao, C. F. Wang, H. C. Lin, H. Chou, and F. Chang, "Tuning the surface free energy of polybenzoxazine thin films," *Journal of Physical Chemistry C*, vol. 112, no. 42, pp. 16189–16191, 2008.

[41] C. F. Wang, S. F. Chiou, F. H. Ko et al., "Polybenzoxazine as a mold-release agent for nanoimprint lithography," *Langmuir*, vol. 23, no. 11, pp. 5868–5871, 2007.

[42] J. A. Macko and H. Ishida, "Behavior of a bisphenol-a-based polybenzoxazine exposed to ultraviolet radiation," *Journal of Polymer Science B*, vol. 38, no. 20, pp. 2687–2701, 2000.

[43] J. A. Macko and H. Ishida, "Structural effects of amines on the photooxidative degradation of polybenzoxazines," *Polymer*, vol. 42, no. 15, pp. 6371–6383, 2001.

[44] W. Hou and Q. Wang, "UV-driven reversible switching of a polystyrene/titania nanocomposite coating between superhydrophobicity and superhydrophilicity," *Langmuir*, vol. 25, no. 12, pp. 6875–6879, 2009.

[45] W. Hou and Q. Wang, "From superhydrophilicity to superhydrophobicity: the wetting behavior of a methylsilicone/phenolic resin/silica composite surface," *Langmuir*, vol. 23, no. 19, pp. 9695–9698, 2007.

[46] K. W. Huang and S. W. Kuo, "High-performance polybenzoxazine nanocomposites containing multifunctional POSS cores presenting vinyl-terminated benzoxazine groups," *Macromolecular Chemistry and Physics*, vol. 211, no. 21, pp. 2301–2311, 2010.

[47] S. W. Kuo and W. C. Liu, "Synthesis and characterization of a cured epoxy resin with a benzoxazine monomer containing allyl groups," *Journal of Applied Polymer Science*, vol. 117, no. 6, pp. 3121–3127, 2010.

[48] K. Wozniak, H. He, J. Klinowski, T. L. Barr, and P. Milart, "ESCA and solid-state NMR studies of ionic complexes of 1,8-bis(dimethylamino)naphthalene," *Journal of Physical Chemistry*, vol. 100, no. 27, pp. 11420–11426, 1996.

[49] K. Wozniak, H. He, J. Klinowski, W. Jones, and T. L. Barr, "ESCA, solid-state NMR, and X-ray diffraction monitor the hydrogen bonding in a complex of 1,8-bis(dimethylamino)naphthalene with 1,2-dichloromaleic acid," *Journal of Physical Chemistry*, vol. 99, no. 40, pp. 14667–14677, 1995.

[50] F. M. Chang, S. J. Hong, Y. J. Sheng, and H. K. Tsao, "High contact angle hysteresis of superhydrophobic surfaces: hydrophobic defects," *Applied Physics Letters*, vol. 95, no. 6, Article ID 064102, 2009.